Sensors and Actuators: A. Physical 333 (2021) 113270

Contents lists available at ScienceDirect

Sensors and Actuators: A. Physical

journal homepage: www.elsevier.com/locate/sna

Dielectric-elastomer-enhanced triboelectric nanogenerator with amplified outputs

Ahmed Haroun[a,*], Chengkuo Lee[b,c,d]

[a] Department of Mechanical Design & Production Engineering, Cairo University, Giza, Egypt
[b] Department of Electrical and Computer Engineering, National University of Singapore, Singapore, Singapore
[c] Center for Intelligent Sensors and MEMS (CISM), National University of Singapore, Singapore
[d] NUS Suzhou Research Institute (NUSRI), Suzhou Industrial Park, Suzhou, People's Republic of China

ARTICLE INFO

Article history:
Received 21 August 2021
Received in revised form 29 October 2021
Accepted 30 November 2021
Available online 3 December 2021

Keywords:
Dielectric elastomer
Triboelectric
Contact electrification
Hybrid
Motion energy harvesting

ABSTRACT

Dielectric elastomers are effective ambient motion energy harvesters due to their flexibility, high energy density, and their ability to match low frequency unsteady motions. However, the dielectric elastomer generator (DEG) is in reality a charge pump, which requires an external supply of electrical charge to work as an energy harvester. In this work, the DEG is coupled with a contact-mode triboelectric nanogenerator (TENG) to form a hybrid. The TENG autonomously produces charges by contact electrification and the DEG in turn amplifies the electrical output by raising the charges to a higher electrical potential. In addition, dielectric elastomer exhibits dielectric strength two orders of magnitude higher than air, thus enabling delivery of a higher output voltage than that by TENG only. Both the TENG and the DEG converts mechanical motion to electrical energy via capacitance change. This makes them physically compatible for easy integration. We first analyze the coupled system and identify the optimal conditions that maximizes output yield in the shortest amount of time. We found that, the maximum output was realized when the TENG and DEG were excited perfectly out-of-phase for same input frequency. We showed that the DEG is ideally able to amplify the voltage output from TENG that is proportional to the capacitance change ratio of the DEG. By the same token, the maximum power will also be amplified proportionally for a constant current system. Our experiment showed that 260% and 180% DEG capacitance change can produce saturation voltage amplification of 2.7 and 2, respectively. Our work demonstrated dielectric-elastomer-enhanced output of a TENG and presented the optimal conditions for maximal amplification.

1. Introduction

Dielectric elastomers (DE) have been shown to exhibit high energy density [1], with theoretical figures of above 1 J/g, and at least 0.7 J/g in optimized experiments [1–3]. Conversion efficiencies of DE generators lie in the range of a few percent and up to 30%, which is dependent on the speed of operation and the mode of deformation [4]. DE generators also exhibit good impedance matching owing to their stretchable nature and are low cost and lightweight [1,5,6]. The key differentiating factors that DE has over conventional electromechanical transducers are its high dielectric strength, high stretchability and the capability of undergoing capacitance change of above 1000 times [4]. Such factors allow DEs to deliver output yields of at least one order of magnitude higher than existing technologies [7,8].

However, the central obstacle that is preventing DE generators from widespread deployment and commercialization is its inability to generate electric charge by mechanical stimulus alone; it requires polarization charges from an external source. Previous works on DE generator development have often been focused on tethering DEGs to a priming source. The need for a high voltage priming source presents further barriers due to user safety and the bulkiness of the source [9–11]. The closest that DE generators come to large-scale deployment is the introduction of a self-priming circuit [12–14]. The self-priming circuit picks up small amounts of charge from a low voltage source, for instance, a battery, and then circulates the charges between itself and the DE generator, in order for the electrical charges to be raised to a sufficiently high potential that realizes the promise of a high energy output. However, a DE generator tethered to a self-priming circuit still requires an external battery and the priming circuit itself, which are often still too bulky to be

* Correspondence to: Dept. of Mechanical Design and Production Engineering, Cairo University, 12613 Egypt.
E-mail address: eng.ahmedharoun@cu.edu.eg (A. Haroun).

https://doi.org/10.1016/j.sna.2021.113270
0924-4247/

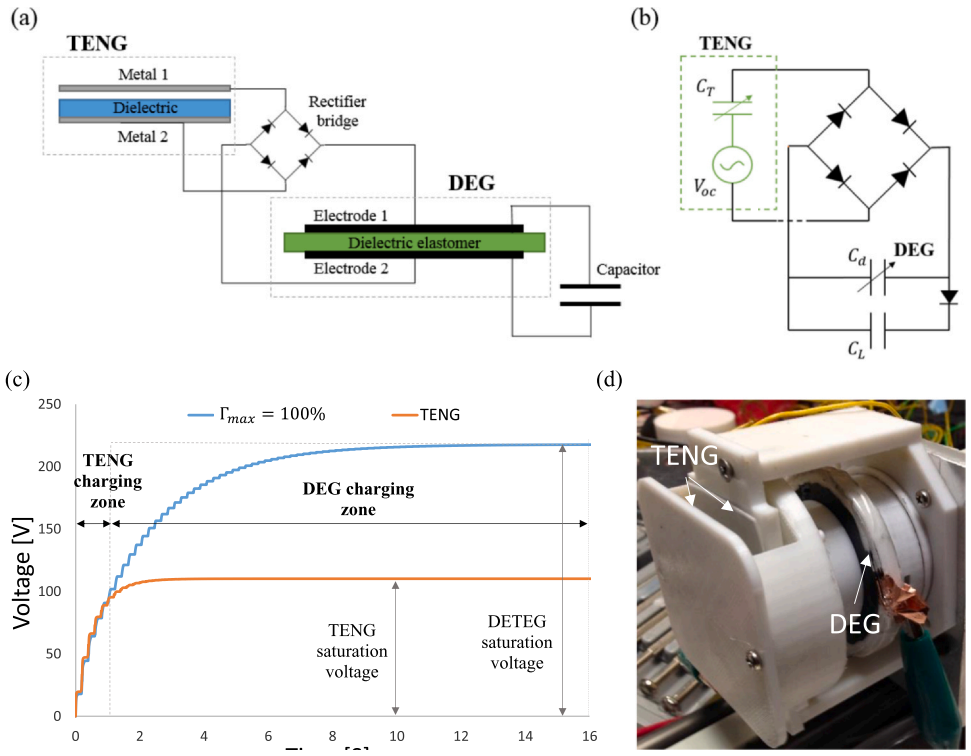

Fig. 1. Contact mode triboelectric nanogenerator (TENG) is coupled with (DEG) to form a dielectric-triboelectric generator (DETEG): (a) Schematic of DETEG; (b) DETEG equivalent circuit modeling; (c) Simulation of the load capacitor voltage while charging by DETEG and TENG systems at (Γ_{max} = 100%). Charging zones and saturation voltages are illustrated. "DEG charging zone" starts at approximately t = 1.25 sec and (d) The DETEG experimental prototype.

used for small-scale applications [15] like that of a human footfall energy harvester. Further developments were made in the form of tethering the DE to electrets [16,17]. However, the need for the electrets to be recharged periodically somewhat diminishes its advantage over autonomous systems like piezoelectrics [18,19] and more recently, triboelectrics [20].

We couple the DE generator with a contact-mode triboelectric generator. We term this the Dielectric-Triboelectric Generator (DETEG). The triboelectric generator, commonly known in its nanogenerator form as Triboelectric Nano-Generator (TENG), is reported with output yields of up to 500 W/m^2 in power flux [21]. This presents a leap in terms of power generation for low frequency motion-based energy harvesting [22,23]. Triboelectric transduction involves the generation of opposite electrostatic charges on two electrically dissimilar surfaces when they come into contact, reminiscent of electrostatic charges generated by friction. Subsequent separation of the surfaces will induce an electric potential across it. Varying the separation distance of the surfaces by mechanical motion will raise the electrical potential, thereby generating electrical energy. TENGs are low-cost, with the ability to effectively scavenge low frequency random motions. TENGs have been demonstrated in many configurations [24,25]. They have also been modeled [26,27] and implemented with some low frequency applications such as to harvest biomechanical [22,23,28] and wind [29] energies.

Although the output voltage of TENG scales with the surface charge density of the contact surfaces, there is a limit on surface charge density [30], as determined by the electric field break down of air between TENG layers that is around 3 MV/m [31,32]. The voltage between TENG layers must be below the air breakdown voltage over the separation distance [30]. For dielectric elastomer generators, the DE membrane has a breakdown strength of one to two orders of magnitude higher than air [33–35]. Thus, a much higher voltage could be sustained across DE membrane. This would make DETEG more suitable with ultra-high voltage applications such as the powering of dielectric elastomer actuators (DEA) [36,37], self-powering of electrospinning systems [38] and plasma generation [39]. In addition, higher voltage provided by the integration of DE with TENG implies a higher output energy and power.

We present a dielectric elastomer generator (DEG) hooked up to a triboelectric nano-generator (TENG) to allow a higher energy density of low frequency ambient motions to be harvested via the voltage amplification of DEG. A contact mode TENG is connected to a DEG via a rectifier bridge, to sustain a positively-biased priming voltage. We connect the DEG to a load capacitor as a simple and practical way to illustrate energy transfer and storage. An input motion to TENG will generate opposite charges on the contact surfaces. These charges set up an electrical potential when the contact surfaces separate from each other. When the electrical potential becomes large enough, electrical charges will be transferred to the DEG via a rectifier bridge (Fig. 1). The electrically-charged DEG will in turn be cyclically-deformed so as to further amplify the electrical potential of the charges. The output charges will then be stored on a load capacitor. We simulate DETEG system using MATLAB/Simulink. MATLAB/Simulink consists of toolboxes that facilitate the modeling of linear and non-linear circuit elements, which are extremely suited to model our TENG and DEG/load capacitor as linear circuit elements, and the diodes as non-linear elements. We use our simulation to determine optimal conditions that maximize voltage amplification and charging speed. We then performed an experiment to verify our simulation results and estimate the output performance of a physical prototype.

2. Mathematical models of TENG and DEG

The voltage of a contact mode triboelectric nanogenerator is given as [40]:

Table 1
Default DETEG parameters used for simulation.

TENG		DEG	
Surface charge density – σ	$40\,\mu C.\,m^{-2}$	Undeformed capacitance – C_o	$1\,nF$
Contact surface area – Z	$0.005\,m^2$	Max. capacitance change Ratio – Γ_{max}	100%
Max. separation distance – x_{max}	$0.002\,m$	Capacitance change frequency – f_D	$5\,Hz$
Input frequency – f_T	$5\,Hz$		
Dielectric layer thickness – d	$100\,\mu m$	Load capacitance – C_L	$10\,nF$
Dielectric constant – ε_r	4		

$$V_T = -\frac{Q}{Z\varepsilon_o}\left(\frac{d}{\varepsilon_r} + x(t)\right) + \frac{\sigma \quad x(t)}{\varepsilon_o} \tag{1}$$

where V_T is the voltage between TENG electrodes, x is the separation distance between triboelectric surfaces, Q is the amount of electrical charge transferred from the TENG through an extend electrical circuit connected to it, σ is the surface charge density of the triboelectric surface pair, Z is the overlap area of the triboelectric layers, and d is the thickness of the dielectric layer. The above equation shows that the voltage on a TENG is equivalent to two circuit elements – an AC voltage source ($V_{oc} = \sigma x/\varepsilon_o$), and a variable capacitor $\left(C_T = \varepsilon_o Z/\left(\frac{d}{\varepsilon_r} + x\right)\right)$ connected in series (Fig. S1a) [28]. The input motion for the TENG is idealized as simple harmonic motion, as shown in Eq. (2) below:

$$x(t) = \frac{x_{max}}{2}(1 - \cos(2\pi f_T t)) \tag{2}$$

where x_{max} is the maximum separation distance between triboelectric surfaces in the TENG and f_T is its harmonic frequency of oscillation.

We couple a dielectric elastomer generator (DEG) to a TENG via bridge rectifier as shown in Fig. 1. A series of mechanical deformation of DEG leads to capacitance change. We define the capacitance at the deformed state as follows:

$$C_D = C_o(1 + \Gamma) \tag{3}$$

where C_o is the capacitance of DEG in an undeformed (reference) state, and C_D is the capacitance in its deformed state, which is time-variant. Hence: $\Gamma = \Delta C_D/C_o$, which is the change in capacitance normalized with its undeformed capacitance, we term the capacitance change ratio. Limiting to only tensile deformation on the elastomer, Γ varies from zero to any prescribed maximum value Γ_{max}.

The magnitude of capacitance change in a DEG depends on the geometrical configuration of the DEG and its amplitude of mechanical deformation [2,4,41,42]. In general, capacitance change may range from a few times its initial capacitance, to more than 1000 times in the equal-biaxial mode of deformation [13,41]. To keep our simulation generic, we consider only the capacitance change magnitude without considering on how the elastomer membrane is stretched. From this, we could obtain the net gain in output voltage and output energy/power from the DEG. We quantify output gain by studying the state of charge of a storage capacitor (C_L) connected to the DETEG (Fig. 1b).

3. Performance optimization of DETEG through simulation

We adopt MATLAB/Simulink physical modeling to simulate the systems of TENG and DETEG. It enables modeling of linear and nonlinear circuit elements easily, which facilities the theoretical analysis and optimal design of TENG and DETEG even with complex electrical systems and power management circuits. Beyond the current study, MATLAB/Simulink enables the integration of TENG and DETEG with other electrical and non-electrical physical systems (ex: mechanical, hydraulic, and pneumatic) as well as simulations with highly varied input signals (by using different Simulink source blocks). Our simulation method may hence be used for the simulation of TENG and DETEG harvesting systems for real applications. See Supplementary information II for details on DETEG system simulation using MATLAB/Simulink.

We benchmarked of our MATLAB simulations with a contact-mode TENG connected to a load capacitor through a bridge rectifier, presented in a previous work [43]. The case was previously simulated using the SPICE (Simulation Program with Integrated Circuit Emphasis). The value of the saturation voltage obtained using MATLAB/Simulink is 105.1 V (Fig. S2b), while that obtained using SPICE was ~ 104.8 V, giving a deviation of less than 1%, which could be attributed to numerical rounding errors.

We study the charging characteristics of a dielectric-triboelectric generator (DETEG) on a load capacitor by simulation. The default parameters used for simulation of both DEG and TENG are listed in Table 1. We again consider simple harmonic motion for the DEG like we did for TENG, with a corresponding sinusoidal temporal variation of DEG's capacitance given by:

$$\Gamma(t) = \frac{\Gamma_{max}}{2}(1 - \cos(2\pi f_D t + \varnothing)) \tag{4}$$

From Eqs. (2) and (4), the initial state of the TENG is when the electro-positive surface (Metal 1 in Fig. 1a) is in full contact with the dielectric, so that $x = 0$ at $t = 0$, and the DEG capacitance will be at its undeformed state at $t = 0$. f_D is the DEG's capacitance variation frequency, while $\varnothing$ is the phase difference between DEG and TENG inputs. From (4), if $\varnothing = 180^o$, then the DEG's capacitance will be at its maximally-stretched state at $t = 0$. To maximize charge transfer from the TENG to the DEG at the start of every charge cycle, we select $\varnothing = 180^o$. We shall subsequently confirm by simulation that this phase difference is optimal to achieve maximal voltage gain by the DEG.

Upon contact, charges will be induced on the TENG by contact electrification. Upon separation, the electrical potential across the TENG will increase and charges will begin to flow to both the DEG and the load capacitor. At the initial state ($t = 0$), we assume there are no charges on both the DEG and the load capacitor. To maintain voltage equilibrium across the TENG, DEG and load capacitor, charges originating from the TENG will be largely absorbed by the load capacitor, since $C_L = 10C_0$. This further implies that the input current into the load capacitor is very much larger than that going into the DEG (Fig. 2e–f). The TENG primarily charges the load capacitor, and the DEG participates minimally in charging the load capacitor (Fig. 2e) as long as $C_L \gg C_D$. Consequently, the TENG bypass the DEG and directly charge load capacitor. As the voltage on the load capacitor equilibrates with the TENG saturation voltage (Fig. 1c), the current flow to the load capacitor will taper off rapidly (Fig. 2f). We term the process described above as the "TENG charging zone".

Once the voltage on the load capacitor equilibrates with the TENG, charges from the TENG will now flow into the DEG. By absorbing charges from the TENG at its high capacitance state, the DEG will push the charges to the load capacitor at a higher potential upon relaxation to its minimum capacitance. The repeated cyclical variation in capacitance of the DEG will progressively raise the voltage on the load capacitor to a higher voltage saturation. We term this new

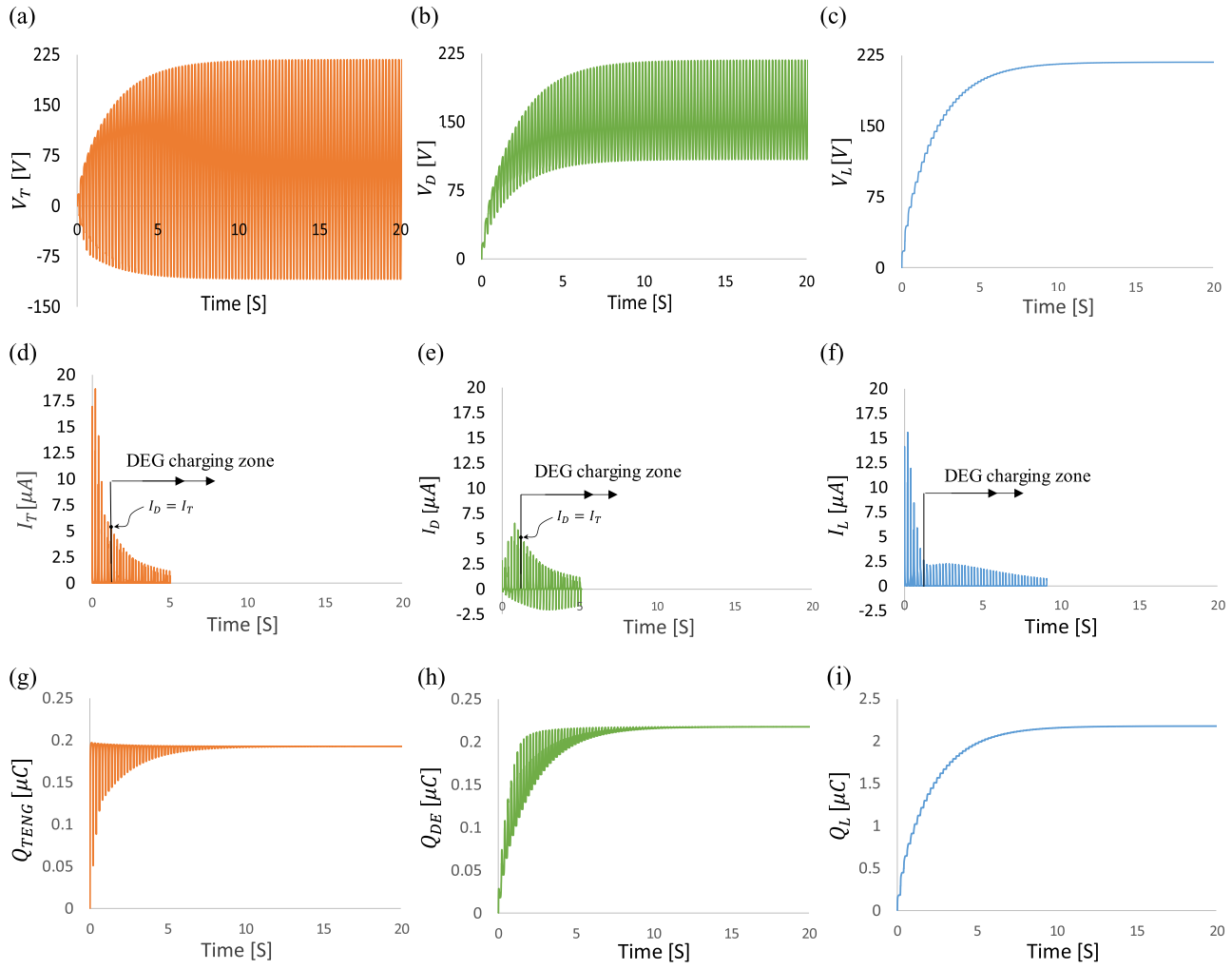

Fig. 2. Simulation of voltage, current, and charge on the three elements of DETEG system. (a) Voltage across TENG before rectifier bridge (b) Voltage across DEG (c) Voltage across C_L (d) Output current from TENG after rectification (e) Input current to DEG. Negative current means output from DEG to C_L (f) Input current to C_L (g) Charge stored on TENG (h) Charge stored on DEG (i) charge stored on C_L.

saturation voltage value as the DETEG saturation voltage (Fig. 1c). The DEG hence acts as a charge pump, amplifying the voltage transferred from the TENG to the load capacitor. We term this process the "DEG charging zone". The "DEG charging zone" commences after the TENG achieves electrical equilibrium with the load capacitor. At the final equilibrium state, all three components will equilibrate at a higher final DETEG saturation voltage (Figs. 1c, 2a–c)) by virtue of dielectric-elastomer-enhanced output of the DEG. When final equilibrium is attained, current flow will taper off to zero (Fig. 2d–f). TENG and DETEG saturation voltages on the load capacitor in our simulation are 110.2 V and 217.8 V, respectively. The saturation voltage is amplified to around twice the TENG saturation voltage with a 100% DEG capacitance change. Consequently, the energy stored on the load capacitor is amplified by 4 times.

3.1. How much DETEG amplifies voltage

The maximum DETEG saturation voltage amplification (α_{max}) depends on the prescribed capacitance change amplitude Γ_{max} (described by Eq. (4)). For a given Γ_{max}, α_{max} may only be attained if all charges from the TENG is transferred to the DEG, and when the DEG is at its maximum capacitance state ($C_{max} = \Gamma_{max}C_0$). The maximum charge ($Q_{max}$) on the DEG may hence be calculated from the case when DEG is fully stretched while being charged by TENG, as follows:

$$Q_{max} = C_0(1 + \Gamma_{max})V_{sat\_TENG} \tag{5}$$

where V_{sat_TENG} is the TENG saturation voltage.

The DETEG saturation voltage (V_{sat_DETEG}) is therefore:

$$V_{sat\_DETEG} = Q_{max}/C_o \tag{6}$$

Eqs. (5) and (6), the maximum saturation voltage amplification (α_{max}) that can be achieved by a given Γ_{max} can be expressed as:

$$\alpha_{max} = \left(\frac{V_{sat\_DETEG}}{V_{sat\_TENG}}\right)_{max} = 1 + \Gamma_{max} \tag{7}$$

Eq. (7) shows a simple linear relationship between α_{max} and Γ_{max}. We shall show in subsequent sections that theoretically, maximum voltage amplification predicted by (7) would only be attained under specific operating conditions, and realistically, it will only be achieved in a lossless circuit.

3.2. Factors affecting DETEG charging performance

When TENG charges a load capacitor, the charging speed depends on the load capacitance (C_L) and the TENG characteristics, while the saturation voltage (V_{sat_TENG}) depends only on the TENG characteristics [23,43]. However, when a TENG charges a load capacitor through a DEG (DETEG), additional factors like the DEG's undeformed capacitance (C_o), maximum capacitance change ratio

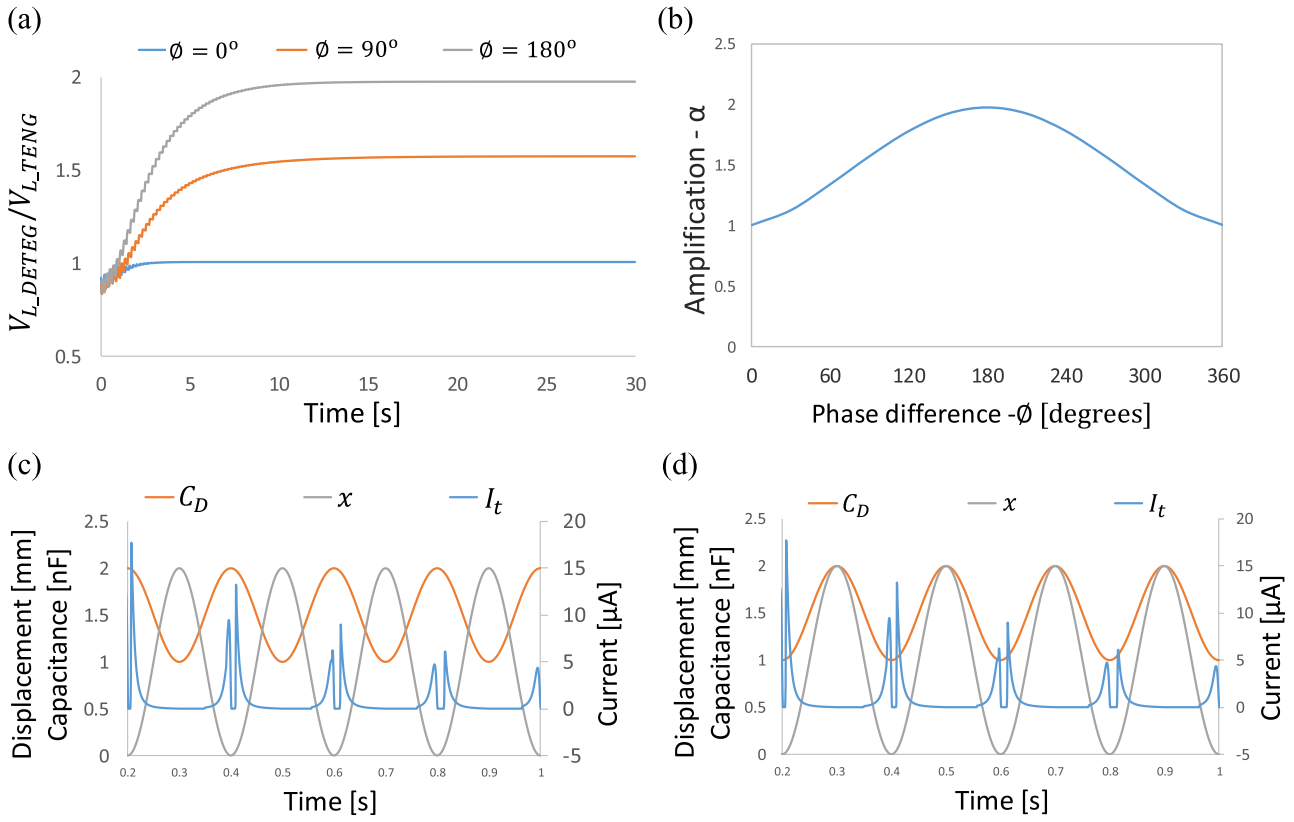

Fig. 3. Effect of phase difference (∅) on the voltage amplification of a DETEG (simulation): (a) Time variation at three levels of ∅; (b) Voltage amplification (α) over one revolution of phase difference; (c) TENG output current along with DEG capacitance and TENG separation distance at ∅ = 180° and (d) at ∅ = 0°.

(Γ_{max}), DEG's operating frequency (f_D) and the phase difference with TENG's input motion (∅) will affect the charging performance on the load capacitor.

3.2.1. Phase difference

Energy harvesting systems usually harvest ambient motion from a single motion source, hence, both the TENG and the DEG will be excited with the same input frequency. However, depending on the physical geometry of the coupled system, a phase difference between their input waves may exist. Fig. 3a shows the normalized voltage on C_L charged by DETEG at three phase differences (∅), with ∅ defined in Eq. (4). The simulation results suggest that the system with 180° out-of-phase excitation gave the maximum voltage amplification (Fig. 3b), consistent with that given by Eq. (7).

Our simulation and previous works [37] showed that the peaks of TENG output current (I_{Tmax}) are generated in the vicinity of the contact state ($x = 0$, Fig. 3c and d), just before and after TENG layers' contact. Hence, in order to maximize the charge transfer to DEG and consequently saturation voltage amplification, one should match the maximum DEG capacitance (C_{Dmax}) to current peaks from the TENG (I_{Tmax}). This synchronization can be easily realized, which we shall demonstrate in our experimental prototype later. Mathematically, from Eqs. (2) and (4), this represents a 180° out-of-phase excitation for the same input frequency (Fig. 3c). Any other values for phase difference will lead to the matching of peak current from the TENG to a lower DEG capacitance, giving a lower voltage amplification (Fig. 3a and b). At the most extreme case of peak current matching with the undeformed capacitance (Fig. 3d), no amplification will take place (Fig. 3a and b).

3.2.2. DEG maximum capacitance change ratio

DEG maximum capacitance change ratio (Γ_{max}) is the main parameter affecting the DEG performance. Higher capacitance change means higher mechanical to electrical energy conversion. Fig. 4a shows the effect of Γ_{max} on the charging behavior and saturation voltage. As suggested by Eq. (7), the saturation voltage increases linearly with Γ_{max} (Fig. 4b), and consequently the storage energy increases in a quadratic manner. We wish to qualify that the quadratic increase in storage energy may further be modified by the DEG operating cycle, bounded by its modes of failure [11,21], DEG configuration and application size dimensions. However, we shall only consider a simplified case of a dielectric-elastomer-enhanced TENG of generic capacitance change, identical excitation frequencies for both the TENG and the DEG in a sinusoidal fashion and with an optimum phase difference (∅ = 180°), so as to focus on the amplification characteristics of a DETEG. Other factors mentioned above will be presented in a separate study.

We express the average power stored in C_L as: $P_{avg} = C_L V_L^2/(2 \times time)$ [23]. P_{avg} increases with the capacitance change ratio as well (Fig. 4c). However, at very low or zero Γ_{max}, maximum P_{avg} of TENG is higher than that of DETEG (Fig. 4d). This is due to the added impedance from the DEG nominal capacitance (C_o) on the circuit in a DETEG system. This introduces an impedance mismatch to the original TENG only circuit, by the DEG, leading to a reduction of maximum power output for the same load capacitor. This power loss is compensated when the DEG is stretched, thereby increasing its capacitance and reducing the overall impedance.

A higher Γ_{max} would also boost the charging power for the same frequency of excitation. This is because, for the same frequency, a higher Γ_{max} would imply a higher rate of change of deformation in

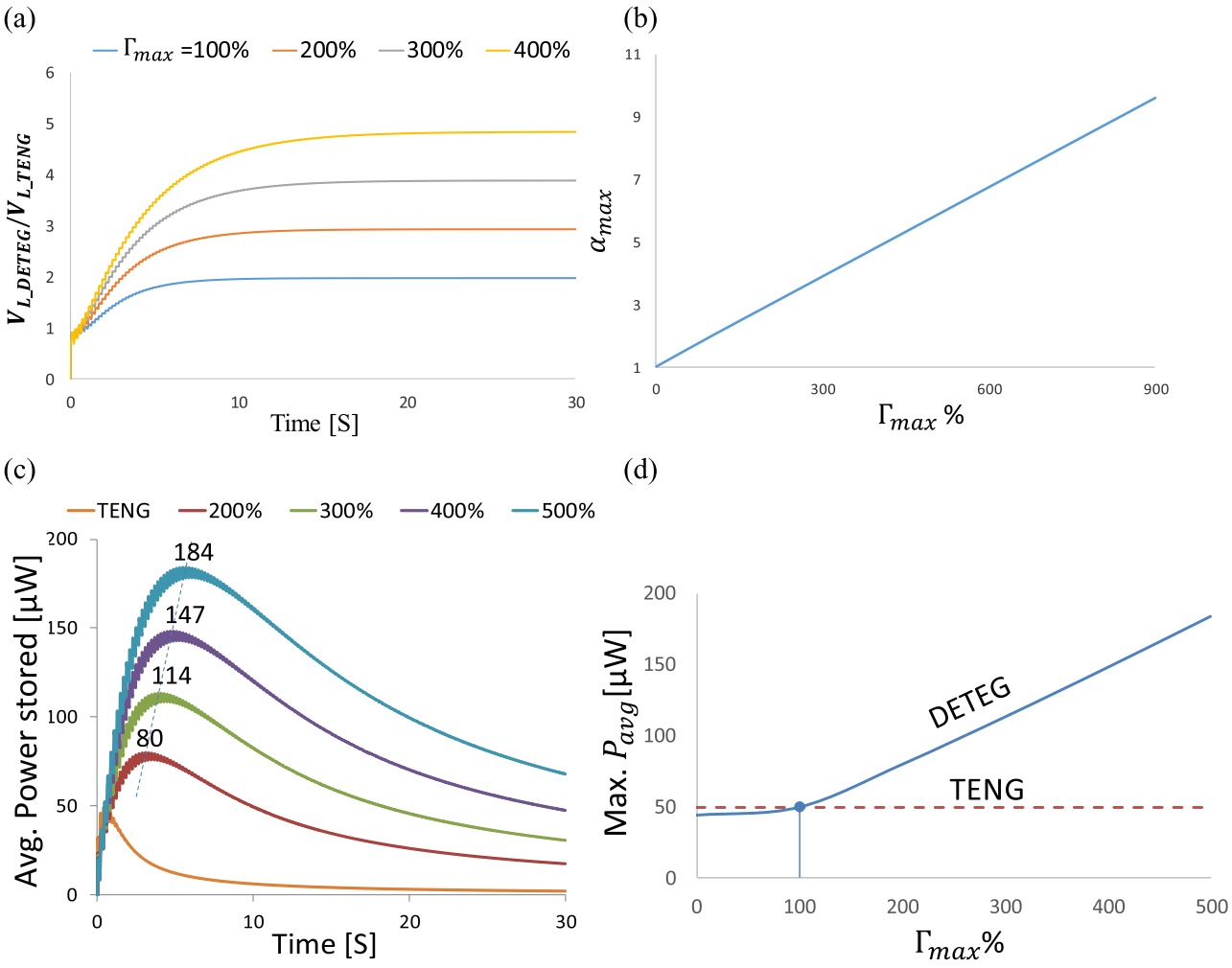

Fig. 4. Amplification and power of a DETEG (simulation): (a) DETEG normalized voltage on load capacitor voltage at different Γ_{max}; (b) Effect of Γ_{max} on the saturation voltage amplification; (c) Average power stored on the load capacitor with time while charging by DETEG at different Γ_{max} (d) Effect of Γ_{max} on DETEG maximum average power transferred to C_L.

the DEG, thereby pumping charges at a higher rate to the load capacitor, giving a higher average power (Fig. 4c and d). The profile of charging power ultimately depends on the transient impedance of all three capacitance components of TENG (C_{Tmax}), DEG ($C_D = C_o + C_o\Gamma_{max}$) and the load capacitor (C_L). In this simulation DETEG maximum P_{avg} exceeds that of TENG with approximately Γ_{max} = 100% (Fig. 4d). DETEG maximum P_{avg} at Γ_{max} = 200% is about 1.6 times (80 µW) that of TENG (49.13 µW), while it is about 4 times (184 µW) at Γ_{max} = 500%. The maximum P_{avg} at Γ_{max} = 0 is 44.11 µW, a little bit less than that of TENG (Fig. 4d).

3.2.3. DEG undeformed capacitance

DEG undeformed capacitance (C_o) affects the impedance contribution towards the DETEG circuit. Hence, it effects the charging power and time to saturation. Unlike a TENG-only circuit, a DETEG circuit effects charge transfer between three capacitors (TENG, DEG, and C_L), with two stages of charging. For instance, in accordance with the maximum power law, the fastest charging speed during "DEG charging zone" can be obtained when the impedance of the three systems matches. However, due to the transient nature of both the TENG and the DEG capacitance (which constantly varies over time), it would be impossible to ensure perfect impedance matching at all times. Furthermore, C_L is usually large compared to the TENG and DEG capacitances, which poses a practical impossibility for impedance matching across all three capacitive components.

Fig. 5a shows the charging behavior of DETEG at different C_o/C_{Tmax}. In case of lowest C_o/C_{Tmax} = 0.1, the combined impedances of DEG and C_L presents the closest match to the TENG impedance (since C_L/C_{Tmax} = 10). Hence, it follows that the DETEG demonstrates highest charging speed during "TENG charging zone", when the deformation of the DEG is participating negligibly in the charging process, whilst charging speed drops during "DEG charging zone", when the current now passes through the deforming DEG. For C_o/C_{Tmax}= 1 and 10, the charging speed during "DEG charging zone" is the highest, indicating good impedance matching between the DETEG components. For C_o/C_{Tmax}= 1, TENG and DEG impedances' are matches, while in case of C_o/C_{Tmax}= 10, the DEG and C_L impedances matches. We illustrate in Fig. 5b and c that, for any given C_L/C_{Tmax} and Γ_{max} there is an optimum C_o/C_{Tmax} that gives the fastest overall charging speed and the highest charging power.

Practically, it is not recommended to use C_L as a direct storage unit of the electrical energy generated by DETEG. Direct connection with a large storage capacitor (for instance, in the order of millifarads) will result in high impedance mismatch, and consequently degradation of the energy transfer and storage efficiency. A design of a power management circuit for DETEG is necessary, in order to guarantee an efficient energy transfer and storage. Similar to the case of only TENG where power management circuits are proposed for the same purpose [23,43]. In one case of TENG power management circuit, a temporary capacitor is inserted between TENG and

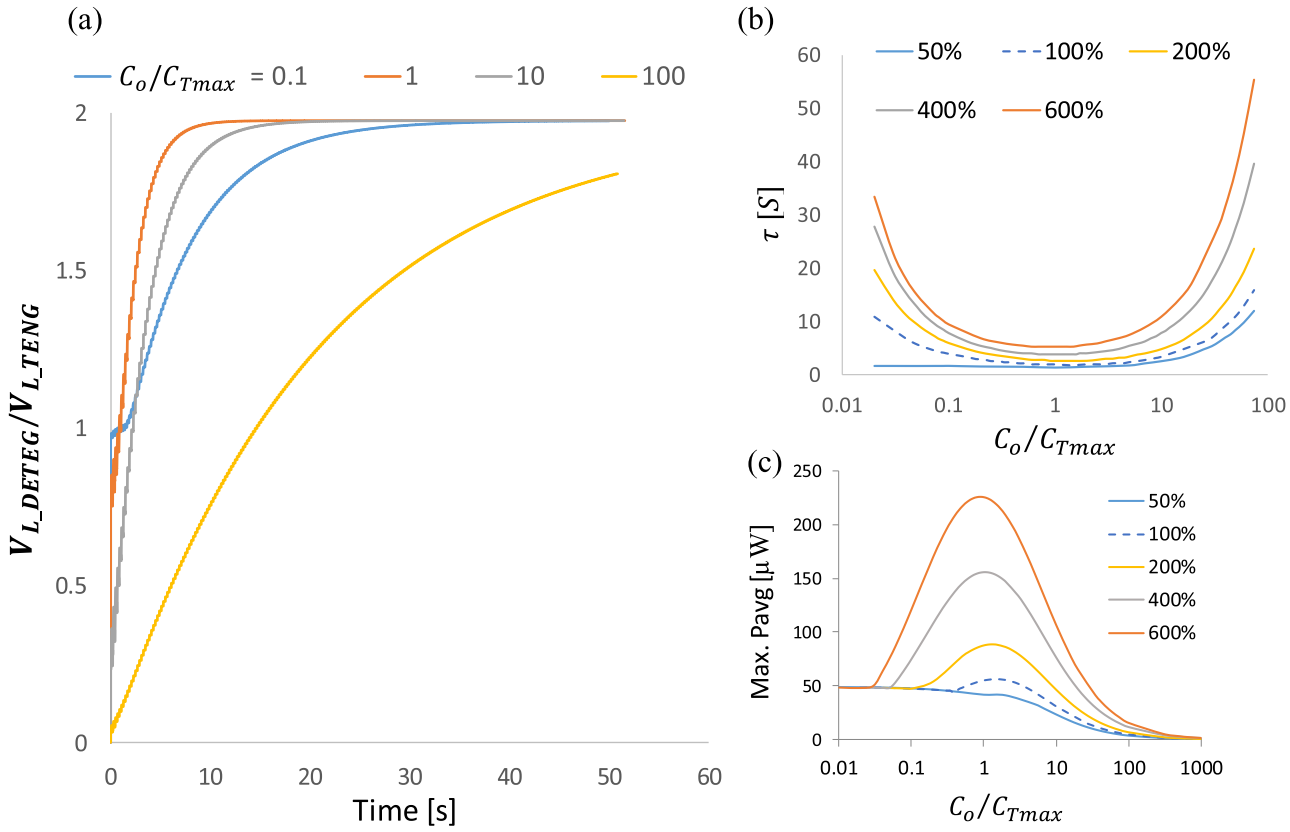

Fig. 5. Relative capacitance between DEG and TENG and its effect on charging speed and power (simulation): (a) DETEG to TENG charging voltage on load capacitor at different DEG undeformed capacitances (C_o); (b) Charging time constant τ versus the capacitance ratio C_o/C_{Tmax} at different Γ_{max}; (c) DETEG max. P_{avg} versus C_o/C_{Tmax} at different Γ_{max}. All graphs are for $C_L/C_{Tmax} = 10$. τ is the charging time required for the voltage to reach 63.2% of the saturation value, which equals to (RC) in the equivalent RC-circuit charged by a DC voltage source.

the storage capacitor. Electronic switches are utilized to allow power transfer between the temporary capacitor and the storage capacitor only when the charging power of the temporary capacitor reaches its maximum value [21].

In the presence of power management circuit between DETEG and the storage unit, C_o needs only to be selected so that TENG and DEG impedances are matching each other and guarantee an efficient energy transfer between them. This is easily achieved, since C_o is usually in the same order of magnitude as C_{Tmax}.

4. Experimental illustrations of amplified outputs and charge transfer efficiency

We perform an experiment to investigate the performance of a DETEG. We compare the experimental results with our simulations to verify our theoretical predications and reveal the sources of deviation. An experimental prototype of size 8 × 7 × 6 cm was fabricated as shown in Fig. 1d and Fig. 6a. It consists of a contact-mode TENG and a ripple configuration DEG [42] (see Supplementary information IV for details of the prototype components, fabrication, and measurements). The sizes of the TENG and DEG assemblies are about D7 × 2 cm, and D5 × 5 cm respectively. The prototype was designed so that both generators undergo the same input displacement from a single input motion source as well as working at the optimum phase difference as suggested by Fig. 3b (TENG layers in contact while the DEG membrane is fully stretched). Ripple configuration is selected for DEG, so that small linear stroke can induce significant capacitance change on the DEG membrane [18] A third-order ripple configuration on the DE membrane was designed by inserting the membrane assembly between two cylindrical cups with three overlapping internal concentric sleeves. The difference in diameter between each sleeve and the corresponding one in the opposite cup is the same for all concentric sleeves, so that the ripple thicknesses would be the same and equally spaced over the membrane. The DEG is an acrylic elastomer VHB4905 membrane, pre-stretched to 1.5 times its original diameter, with carbon grease used as its electrodes.

We provide the linear input motion to the prototype by a linear actuator, which consists of a stepping motor attached to a linear guide through a flexible coupling. The stepping motor has 1 N.m holding torque to be able to provide sufficient compression in the prototype. The motor has 4 wires connections and controlled by MATLAB through an Arduino chip. We vary Γ_{max} by changing the internal allowable displacement in the prototype using different height spacers (Fig. 6a). Changing of this displacement will be reflected on TENG input amplitude (x_{max}) as well. However, the charging behavior of contact-mode TENG is almost independent of x_{max} [43,44].

Fig. 6b shows the charging behavior of a load capacitor of 4.2 nF by a contact-mode TENG and DETEG (see Supplementary movie). Average saturation voltage amplification by the DETEG for each Γ_{max} was obtained from four independent samples. Average saturation voltages of 325 V, 305 V, 245 V, and 187 V are obtained at Γ_{max} of 260%, 220%, 180%, and 104% respectively, while the average saturation voltage of TENG only was 122 V. This gave us voltage amplifications ranging between 1.5 and 2.7. These figures differ from the lossless system suggested in Eq. (7) because in reality, charge transfer from the TENG to DEG and load capacitor will suffer from circuit and current leakage losses, as well as mechanical viscous losses in the DEG [4].

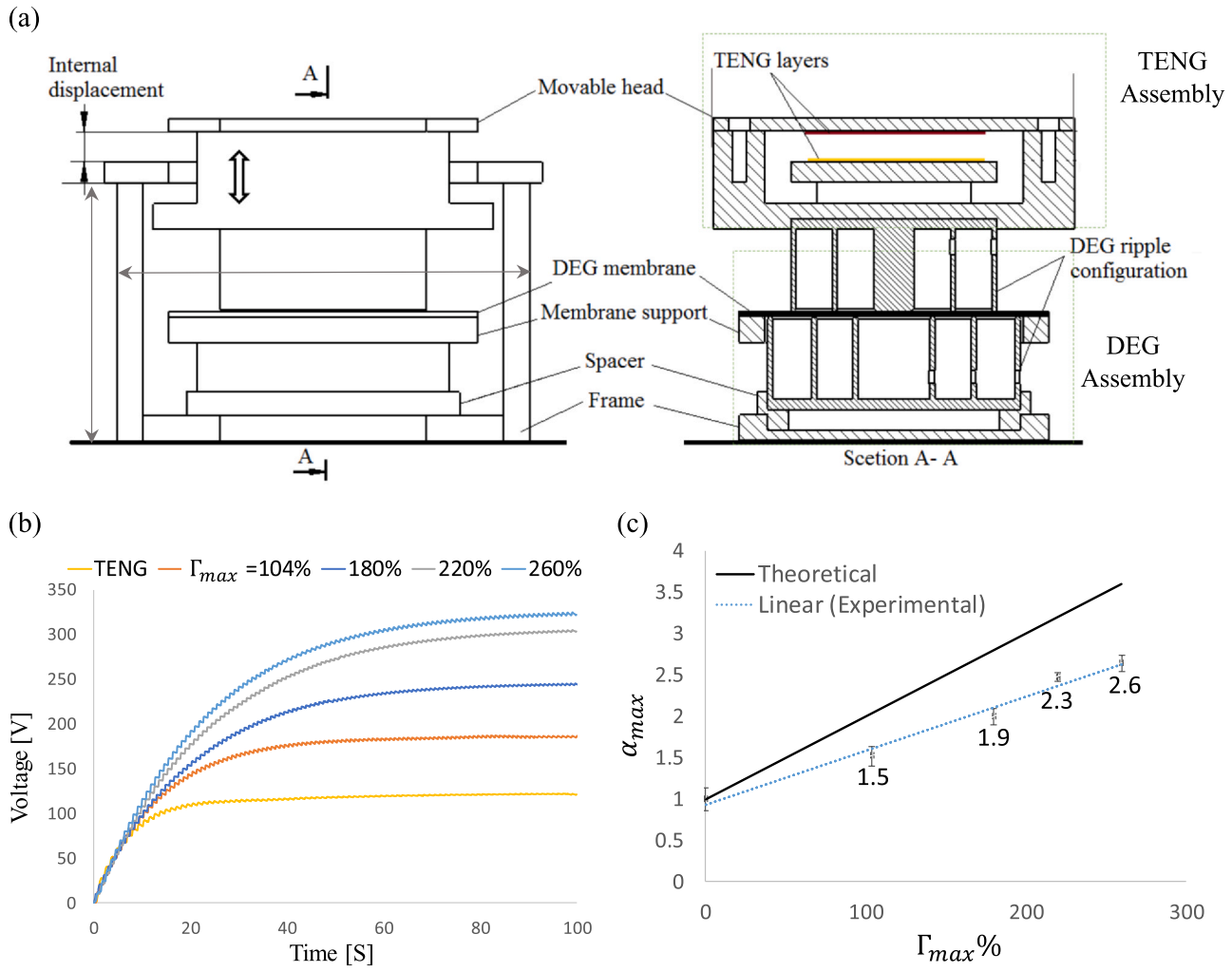

Fig. 6. Performance of a dielectric-triboelectric generator (DETEG) prototype: (a) Prototype drawing. Front view of the prototype presented on the left that shows the overall profile of the prototype. A cross-sectional view presented on the right that shows the details of the TENG and DEG; (b) Voltage on the load capacitor with time while charged by TENG and DETEG at four levels of capacitance change ratios Γ_{max}; (c) Experimental saturation voltage amplification with Γ_{max} along with the theoretical trend. Four DETEG samples are tested at each Γ_{max} value, where the maximum, minimum, and mean values are indicated at every experimental data point.

Supplementary material related to this article can be found online at doi:10.1016/j.sna.2021.113270.

We compute the energy stored in the load capacitor while charging by TENG only and DETEG (at Γ_{max}= 260%) to be 0.03 mJ, and 0.2 mJ respectively. DETEG can charge the capacitor with one order of magnitude energy higher than TENG. Regarding the energy density, TENG of D7 × 2 cm size offers 0.39 J/m^3, while DETEG of total 8 × 7 × 6 cm size offers 0.6 J/m^3. This is an advantage of DETEG system. If there is an available mechanical energy to sufficiently deform the elastomer membrane, DETEG can offer higher energy density than TENG only. Fig. 6c shows the experimental values of voltage amplification at different Γ_{max} along with the theoretical predicated values. Our experiment shows a strong correlation between DETEG voltage amplification (α) and the DEG capacitance change ratio (Γ_{max}). In an ideal, lossless system, the gradient of the $\alpha - \Gamma_{max}$ line should be 1, in accordance with Eq. (7). In reality, due to imperfect charge transfer and energy losses in the system, for instance charge leakage from the DEG and load capacitor, diode current backflow, non-Ohmic losses and mechanical viscosity, the fitted gradient will be less than 1. We propose the usage of this fitted gradient as a measure of overall charge transfer efficiency for a DETEG circuit (γ). In this work, we have γ= 65%.

5. Conclusion

We use a dielectric elastomer generator (DEG) to amplify the output of a triboelectric nanogenerator (TENG), which we termed the dielectric-triboelectric generator (DETEG). We used theory to determine the limits of voltage amplification of DETEG and identified optimal conditions for this amplification to be maximized. We further analyzed a DETEG and showed that the time-to-saturation on the load capacitor is minimized when impedance is matched between the TENG and the DEG, while maximum average power may not be absolutely maximized due to the transient nature of both TENG and DEG. We have, however, produced a plot that gives optimal ratios between the undeformed capacitance of the DEG, with the maximum capacitance of the TENG that maximizes the output power for a given capacitance change ratio of a DEG. This maximum always differs from the matching impedance between an undeformed DEG and the maximum capacitance of the TENG as the load capacitance is realistically much larger than both the DEG and TENG. We established a simple linear relationship between the maximum voltage amplification and the capacitance change ratio (Eq. (7)) and used it as a reference to measure charge transfer efficiency of a real DETEG. Our experiments show that voltage

amplification ranges between 1.5 and 2.7 when the capacitance change ratio varies between 104% and 260%. The charge transfer efficiency is about 65%. In fact, the main feature of DETEG is the high output voltage. Thus, it can be very suitable with high voltage applications such as powering of dielectric elastomer actuators (DEA) and self-powering of electrospinning systems. In addition, DETEG can show an increase in the energy density over only-TENG when there is an available input mechanical energy to make sufficient deformation of the DEG membrane. We have established a method to analyze DETEG, and identified optimal conditions where voltage, time-to-saturation, energy and output power could be maximized. Our work has shown the ability of DEG to amplify output from a TENG, which heralds the future development of compact, high-powered motion-based energy harvesters.

CRediT authorship contribution statement

Ahmed Haroun: Conceptualization, Methodology, Software, Validation, Investigation, Data curation, Writing – original draft, Visualization. **Chengkuo Lee:** Conceptualization, Methodology, Supervision, Writing – review & editing, Resources**,** Visualization.

Declaration of Competing Interest

The authors declare that they have no known competing financial interests or personal relationships that could have appeared to influence the work reported in this paper.

Acknowledgement

The authors deeply acknowledge the valuable comments and advice of Dr. Adrian Koh for conducting experiments on dielectric elastomers.

Appendix A. Supporting information

Supplementary data associated with this article can be found in the online version at doi:10.1016/j.sna.2021.113270.

References

[1] R. Pelrine, R.D. Kornbluh, J. Eckerle, P. Jeuck, S. Oh, Q. Pei, S. Stanford, Dielectric elastomers: generator mode fundamentals and applications, Proc. SPIE (2001) 148–156.
[2] S.J.A. Koh, C. Keplinger, T. Li, S. Bauer, Z. Suo, Dielectric elastomer generators: how much energy can be converted? IEEE/ASME Trans. Mechatron. 16 (2011) 33–41.
[3] S. Shian, J. Huang, S. Zhu, D.R. Clarke, Optimizing the electrical energy conversion cycle of dielectric elastomer generators, Adv. Mater. 26 (2014) 6617–6621.
[4] J. Huang, S. Shian, Z. Suo, D.R. Clarke, Maximizing the energy density of dielectric elastomer generators using equi-biaxial loading, Adv. Funct. Mater. 23 (2013) 5056–5061.
[5] Z. Suo, Theory of dielectric elastomers, Acta Mech. Solid. Sin. 23 (2010) 549–578.
[6] R. Pelrine, R. Kornbluh, Q. Pei, J. Joseph, High-speed electrically actuated elastomers with strain greater than 100%, Science 287 (2000) 836–839.
[7] A. Haroun, I. Yamada, Study of electromagnetic vibration energy harvesting with free/impact motion for low frequency operation, J. Sound Vib. 349 (2015) 389–402.
[8] A. Haroun, I. Yamada, S. Warisawa, Investigation of kinetic energy harvesting from human body motion activities using free/impact based micro electromagnetic generator, Diabetes Cholest. Metab. 1 (2016) 13–16.
[9] C. Jean-Mistral, S. Basrour, J.-J. Chaillout, Dielectric polymer: scavenging energy from human motion, Electroactive Polymer Actuators and Devices (EAPAD) 2008, International Society for Optics and Photonics 2008, p. 692716.
[10] J. Maas, C. Graf, Dielectric elastomers for hydro power harvesting, Smart Mater. Struct. 21 (2012) 064006.
[11] P. Jean, A. Wattez, G. Ardoise, C. Melis, R. Van Kessel, A. Fourmon, E. Barrabino, J. Heemskerk, J.P. Queau, Standing wave tube electro active polymer wave energy converter, Proc. SPIE (2012) 83400C.
[12] T. McKay, B. O'Brien, E. Calius, I. Anderson, An integrated, self-priming dielectric elastomer generator, Appl. Phys. Lett. 97 (2010) 062911.
[13] T.G. McKay, B.M. O'Brien, E.P. Calius, I.A. Anderson, Soft generators using dielectric elastomers, Appl. Phys. Lett. 98 (2011) 142903.
[14] P.K. Illenberger, U.K. Madawala, I.A. Anderson, Big power from walking, Electroactive Polymer Actuators and Devices (EAPAD) 2016, International Society for Optics and Photonics 2016, p. 97980V.
[15] A. Haroun, Xianhao Le, Shan Gao, Bowei Dong, Tianyiyi He, Zixuan Zhang, Feng Wen, Siyu Xu, Chengkuo Lee, Progress in micro/nano sensors and nanoenergy for future AIoT-based smart home applications, Nano Express 2 (2021) 022005.
[16] C. Jean-Mistral, T. Vu Cong, A. Sylvestre, Advances for dielectric elastomer generators: replacement of high voltage supply by electret, Appl. Phys. Lett. 101 (2012) 162901.
[17] T. Vu-Cong, C. Jean-Mistral, A. Sylvestre, Electrets substituting external bias voltage in dielectric elastomer generators: application to human motion, Smart Mater. Struct. 22 (2013) 025012.
[18] A.T. Mathew, V.T.V. Khanh, M.D. Bin Mohamed Aliffi, C. Liu, S.J.A. Koh, A self-amplifying dielectric-elastomer-amplified piezoelectric for motion-based energy harvesting, J. Intell. Mater. Syst. Struct. 31 (2020) 152–166.
[19] A.T. Mathew, C. Liu, T.Y.N. Ng, S.J.A. Koh, A high energy dielectric-elastomer-amplified piezoelectric (DEAmP) to harvest low frequency motions, Sens. Actuators A: Phys. 294 (2019) 61–72.
[20] Z.L. Wang, J. Chen, L. Lin, Progress in triboelectric nanogenerators as a new energy technology and self-powered sensors, Energy Environ. Sci. 8 (2015) 2250–2282.
[21] Y. Wang, Y. Yang, Z.L. Wang, Triboelectric nanogenerators as flexible power sources, npj Flex. Electron. 1 (2017) 10.
[22] P. Bai, G. Zhu, Z.-H. Lin, Q. Jing, J. Chen, G. Zhang, J. Ma, Z.L. Wang, Integrated multilayered triboelectric nanogenerator for harvesting biomechanical energy from human motions, ACS Nano 7 (2013) 3713–3719.
[23] S. Niu, X. Wang, F. Yi, Y.S. Zhou, Z.L. Wang, A universal self-charging system driven by random biomechanical energy for sustainable operation of mobile electronics, Nat. Commun. 6 (2015) 8975.
[24] S. Niu, Y. Liu, S. Wang, L. Lin, Y.S. Zhou, Y. Hu, Z.L. Wang, Theoretical investigation and structural optimization of single-electrode triboelectric nanogenerators, Adv. Funct. Mater. 24 (2014) 3332–3340.
[25] S. Niu, Y. Liu, X. Chen, S. Wang, Y.S. Zhou, L. Lin, Y. Xie, Z.L. Wang, Theory of freestanding triboelectric-layer-based nanogenerators, Nano Energy 12 (2015) 760–774.
[26] S. Niu, Z.L. Wang, Theoretical systems of triboelectric nanogenerators, Nano Energy 14 (2015) 161–192.
[27] M.D. Swartz, T. Kim, J. Niu, R.K. Yu, S. Shete, I. Ionita-Laza, Simulation method for optimizing the performance of an integrated triboelectric nanogenerator energy harvesting system, Nano Energy 8 (2014) 150–156.
[28] F.A. Hassani, Q. Shi, F. Wen, T. He, A. Haroun, Y. Yang, Y. Feng, C. Lee, Smart materials for smart healthcare–moving from sensors and actuators to self-sustained nanoenergy nanosystems, Smart Mater. Med. 1 (2020) 92–124.
[29] Y. Yang, G. Zhu, H. Zhang, J. Chen, X. Zhong, Z.-H. Lin, Y. Su, P. Bai, X. Wen, Z.L. Wang, Triboelectric nanogenerator for harvesting wind energy and as self-powered wind vector sensor system, ACS Nano 7 (2013) 9461–9468.
[30] S. Wang, Y. Xie, S. Niu, L. Lin, C. Liu, Y.S. Zhou, Z.L. Wang, Maximum surface charge density for triboelectric nanogenerators achieved by ionized-air injection: methodology and theoretical understanding, Adv. Mater. 26 (2014) 6720–6728.
[31] P.A. Tipler, College Physics: Worth Pub, 1987.
[32] Sa Schuster, Macmillan encyclopedia of physics, Macmillan Encyclopedia of Physics (Book 1), first ed., Macmillan Library Reference, 1996, p. 1881.
[33] B. Chen, M. Kollosche, M. Stewart, J. Busfield, F. Carpi, Electrical breakdown of an acrylic dielectric elastomer: effects of hemispherical probing electrode's size and force, Int. J. Smart Nano Mater. 6 (2015) 290–303.
[34] B. Chen, M. Kollosche, M. Stewart, J. Busfield, F. Carpi, Electrical breakdown of dielectric elastomers: influence of compression, electrode's curvature and environmental humidity, Electroactive Polymer Actuators and Devices (EAPAD) 2016, International Society for Optics and Photonics 2016, p. 97980Q.

[35] M. Yamada, Y. Murakami, T. Kawashima, M. Nagao, Electrical breakdown of dielectric elastomer and its lamination effect, in: Proceedings of the Electrical Insulation and Dielectric Phenomena (CEIDP), 2014 IEEE Conference on, IEEE 2014, pp. 126–9.
[36] X. Chen, T. Jiang, Y. Yao, L. Xu, Z. Zhao, Z.L. Wang, Stimulating acrylic elastomers by a triboelectric nanogenerator–toward self-powered electronic skin and artificial muscle, Adv. Funct. Mater. 26 (2016) 4906–4913.
[37] L. Xu, H. Wu, G. Yao, L. Chen, X. Yang, B. Chen, X. Huang, W. Zhong, X. Chen, Z. Yin, Z.L. Wang, Giant voltage enhancement via triboelectric charge supplement channel for self-powered electroadhesion, ACS Nano 12 (2018) 10262–10271.
[38] C. Li, Y. Yin, B. Wang, T. Zhou, J. Wang, J. Luo, W. Tang, R. Cao, Z. Yuan, N. Li, X. Du, C. Wang, S. Zhao, Y. Liu, Z.L. Wang, Self-powered electrospinning system driven by a triboelectric nanogenerator, ACS Nano 11 (2017) 10439–10445.
[39] J. Cheng, W. Ding, Y. Zi, Y. Lu, L. Ji, F. Liu, et al., Triboelectric microplasma powered by mechanical stimuli, 9, 2018, 3733.
[40] S. Niu, S. Wang, L. Lin, Y. Liu, Y.S. Zhou, Y. Hu, Z.L. Wang, Theoretical study of contact-mode triboelectric nanogenerators as an effective power source, Energy Environ. Sci. 6 (2013) 3576–3583.
[41] R. Pelrine, R. Kornbluh, Dielectric elastomers as electroactive polymers (EAPs): fundamentals, Electro Act. Polym. (2016) 671–686.
[42] J. Huang, S. Shian, Z. Suo, D.R. Clarke, Dielectric Elastomer Generator with Equibiaxial Mechanical Loading for Energy Harvesting, Society of Photo-Optical Instrumentation Engineers (SPIE), (2013).
[43] S. Niu, Y. Liu, Y.S. Zhou, S. Wang, L. Lin, Z.L. Wang, Optimization of triboelectric nanogenerator charging systems for efficient energy harvesting and storage, IEEE Trans. Electron Devices 62 (2015) 641–647.
[44] Y. Zi, J. Wang, S. Wang, S. Li, Z. Wen, H. Guo, Z.L. Wang, Effective energy storage from a triboelectric nanogenerator, Nat. Commun. 7 (2016) 10987.

Ahmed Haroun received his BSc and MSc degrees in Mechanical Design and Production Engineering from Cairo University in 2008, and 2011 respectively. He received his Ph.D. degree in Mechanical Engineering from University of Tokyo in 2015. From 2015 to 2020, he has been working as a research fellow at National University of Singapore. He is currently an Assistant Professor at The Department of Mechanical Design and Production Engineering, Cairo University.

Chengkuo Lee received his Ph.D. degree in Precision Engineering from The University of Tokyo in 1996. Currently, he is the director of Center for Intelligent Sensors and MEMS at National University of Singapore, Singapore. In 2001, he cofounded Asia Pacific Microsystems, Inc., where he was the Vice President. From 2006 to 2009, he was a Senior Member of the Technical Staff at the Institute of Microelectronics, A-STAR, Singapore. He has contributed to more than 380 peer-reviewed international journal articles. His ORCID is 0000-0002-8886-3649.